

13. Smith, S. B., Cui, Y. & Bustamante, C. Overstretching B-DNA: the elastic response of individual double-stranded and single-stranded DNA molecules. *Science* **271**, 795–799 (1996).

14. Rief, M., Fernandez, J. M. & Gaub, H. E. Elastically coupled two-level-systems as a model for biopolymer extensibility. *Phys. Rev. Lett.* **81**, 4764–4767 (1998).

15. Brown, G. M. & Levy, H. A. α -D-Glucose: precise determination of crystal and molecular structure by neutron-diffraction analysis. *Science* **147**, 1038–1039 (1965).

16. Chu, S. C. C. & Jeffrey, G. A. The refinement of the crystal structures of β -D-glucose and cellobiose. *Acta Crystallogr. B* **24**, 830–838 (1968).

17. Brown, G. M. & Levy, H. A. α -D-Glucose: further refinement based on neutron-diffraction data. *Acta Crystallogr. B* **35**, 656–659 (1979).

18. Brady, J. W. Molecular dynamics simulations of α -D-glucose. *J. Am. Chem. Soc.* **108**, 8153–8160 (1986).

19. Brady, J. W. Molecular dynamics simulations of β -D-glucopyranose. *Carbohydr. Res.* **165**, 306–312 (1987).

20. Joshi, N. V. & Rao, V. S. R. Flexibility of the pyranose ring in α - and β -D-glucoses. *Biopolymers* **18**, 2993–3004 (1979).

21. Bobbitt, J. M. in *Advances in Carbohydrate Chemistry* (eds Wolfram, M. L. & Tipson, R. S.) 1–4 (Academic, New York, 1956).

22. Smith, S. B., Finzi, L. & Bustamante, C. Direct mechanical measurements of the elasticity of single DNA molecules by using magnetic beads. *Science* **258**, 1122–1126 (1992).

23. Li, H., Rief, M., Oesterhelt, F. & Gaub, H. E. Single-molecular force spectroscopy on xanthan by AFM. *Adv. Mater.* **3**, 316–319 (1998).

24. Kellie, G. M. & Riddell, F. G. Non-chair conformations of six-membered rings. *Top. Stereochem.* **8**, 225–264 (1974).

25. Pickett, H. M. & Strauss, H. L. Conformational structure, energy, and inversion rates of cyclohexane and some related oxanes. *J. Am. Chem. Soc.* **92**, 7281–7290 (1970).

26. Drickamer, K. Making a fitting choice: common aspects of sugar-binding sites in plant and animal lectins. *Structure* **5**, 465–468 (1997).

27. Barton, D. H. R. The principles of conformational analysis. *Science* **169**, 539–544 (1970).

28. Florin, E. L. et al. Sensing specific molecular interactions with the atomic force microscope. *Biosensors Bioelectr.* **10**, 895–901 (1995).

29. Quant97/CHARMm (Molecular Simulations, 9685 Scranton Rd, San Diego, California 92121, USA, 1997).

30. Gaussian 94 (Gaussian Inc., Carnegie Office Prk, Bldg 6, Pittsburgh, Pennsylvania 15106, USA, 1994).

Acknowledgements. This work was supported by the NSF (P.E.M.) and the NIH (J.M.F.).

Correspondence and requests for materials should be addressed to J.M.F. (e-mail: fernandez,julio@mayo.edu).

Effect of interannual climate variability on carbon storage in Amazonian ecosystems

Hanqin Tian*, Jerry M. Melillo*, David W. Kicklighter*, A. David McGuire†, John V. K. Helfrich III*, Berrien Moore III‡ & Charles J. Vörösmarty‡

* The Ecosystems Center, Marine Biological Laboratory, Woods Hole, Massachusetts 02543, USA

† US Geological Survey, Alaska Cooperative Fish and Wildlife Research Unit, University of Alaska, Fairbanks, Alaska 99775, USA

‡ Institute for the Study of Earth, Oceans and Space, University of New Hampshire, New Hampshire 03824, USA

The Amazon Basin contains almost one-half of the world's undisturbed tropical evergreen forest as well as large areas of tropical savanna^{1,2}. The forests account for about 10 per cent of the world's terrestrial primary productivity and for a similar fraction of the carbon stored in land ecosystems^{2,3}, and short-term field measurements⁴ suggest that these ecosystems are globally important carbon sinks. But tropical land ecosystems have experienced substantial interannual climate variability owing to frequent El Niño episodes in recent decades⁵. Of particular importance to climate change policy is how such climate variations, coupled with increases in atmospheric CO₂ concentration, affect terrestrial carbon storage^{6–8}. Previous model analyses have demonstrated the importance of temperature in controlling carbon storage^{9,10}. Here we use a transient process-based biogeochemical model of terrestrial ecosystems^{3,11} to investigate interannual variations of carbon storage in undisturbed Amazonian ecosystems in response to climate variability and increasing atmospheric CO₂ concentration during the period 1980 to 1994. In El Niño years, which bring hot, dry weather to much of the Amazon region, the ecosystems act as a source of carbon to the atmosphere (up to 0.2 petagrams of carbon in 1987 and 1992). In other years, these ecosystems act as a carbon sink (up to 0.7 Pg C in 1981 and

1993). These fluxes are large; they compare to a 0.3 Pg C per year source to the atmosphere associated with deforestation in the Amazon Basin in the early 1990s¹². Soil moisture, which is affected by both precipitation and temperature, and which affects both plant and soil processes, appears to be an important control on carbon storage.

Carbon fluxes calculated using the Terrestrial Ecosystem Model (TEM) include net primary production (NPP), microbial respiration (R_H) and net ecosystem production (NEP), all of which are influenced by climate. Net primary production, the net amount of carbon captured by plants, is also influenced by atmospheric CO₂ concentration. The difference between NPP and R_H equals NEP, which is equivalent to annual net carbon storage or loss for an ecosystem.

For regional or global extrapolations with TEM, we use input data on vegetation, elevation, soil texture, monthly mean temperature, monthly mean precipitation, and monthly mean solar radiation. The input data sets are gridded at a resolution of 0.5° latitude by 0.5° longitude. The structure, parametrization, calibration and performance of TEM have been documented previously^{3,11}.

We first ran TEM in equilibrium mode to generate an initial condition for the transient runs, using the long-term mean of monthly temperature, monthly precipitation, monthly solar radiation and the level of atmospheric CO₂ concentration at the beginning of this century (296 p.p.m.y.). Then we ran TEM in transient mode using historical input data from 1900 to 1994 including: (1) historical mean atmospheric CO₂ concentration generated from atmospheric and ice core CO₂ observations¹³, and (2) historical monthly data for air temperature¹⁴ and precipitation¹⁵. The historical temperature and precipitation data were interpolated by the Max Planck Institute for Meteorology to a 0.5° spatial resolution. Two transient runs were made: one considering the climate and CO₂ transients together, and one considering only the climate transient. A comparison of these two runs was used to determine the effect of CO₂ 'fertilization' on carbon storage. All other model analyses were based on the combined climate and CO₂ transient run. We used the IGBP-DIS land-cover data set¹⁶ as a basis for adjusting the area of undisturbed ecosystems in the Basin to account for land-cover conversions such as forest to cropland. This reduces the area of undisturbed ecosystems by 11%, which is in good agreement with other land-cover change estimates for the Basin^{12,17}.

For the Amazon Basin, TEM results (Table 1) show that annual NEP varied from –0.2 Pg C (10¹⁵ g C) in 1987 and 1992, to 0.7 Pg C in 1981 and 1993, because of the combined effects of climate variability and increasing atmospheric CO₂ concentration. A negative NEP means these ecosystems are a source of atmospheric CO₂,

Table 1 Interannual variations in carbon fluxes in Amazonian ecosystems

Year	Climate with CO ₂			Climate only		
	NPP (Pg C yr ⁻¹)	R_H (Pg C yr ⁻¹)	NEP (Pg C yr ⁻¹)	NPP (Pg C yr ⁻¹)	R_H (Pg C yr ⁻¹)	NEP (Pg C yr ⁻¹)
1980	5.0	4.7	0.3	4.5	4.5	0.0
1981	5.4	4.7	0.7	4.9	4.4	0.5
1982	4.9	4.8	0.1	4.3	4.5	–0.2
1983	4.8	4.9	–0.1	4.2	4.6	–0.4
1984	5.3	4.8	0.5	4.7	4.5	0.2
1985	5.0	4.8	0.2	4.4	4.4	0.0
1986	5.2	4.8	0.4	4.7	4.5	0.2
1987	4.7	4.9	–0.2	4.1	4.6	–0.5
1988	5.0	4.9	0.1	4.3	4.5	–0.2
1989	5.1	4.8	0.3	4.6	4.5	0.1
1990	5.1	4.8	0.3	4.5	4.5	0.0
1991	4.8	4.9	–0.1	4.1	4.5	–0.4
1992	4.6	4.8	–0.2	3.8	4.4	–0.6
1993	5.7	5.0	0.7	5.1	4.5	0.6
1994	5.3	5.0	0.3	4.7	4.6	0.1
s.d.	0.3	0.1	0.3	0.3	0.1	0.3

The carbon fluxes between the atmosphere and undisturbed Amazonian ecosystems in response to interannual climate variability and increasing atmospheric CO₂ concentration as estimated by the Terrestrial Ecosystem Model. NPP, net primary production; R_H , heterotrophic respiration; NEP, net ecosystem production; s.d., standard deviation. A negative NEP indicates a net flux of carbon from the land to the atmosphere.

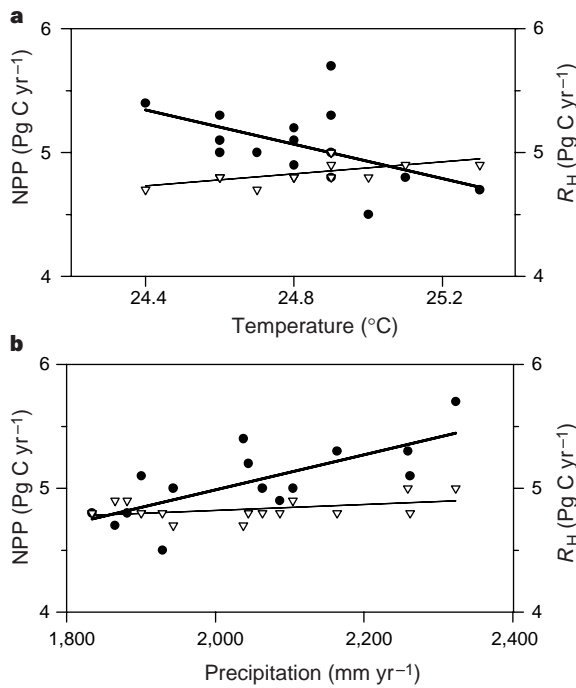


Figure 1 Relation of carbon fluxes to temperature and precipitation. **a**, Relations of annual net primary production (NPP, thick line, circles) and annual heterotrophic respiration (R_H , thin line, triangles) to annual mean temperature in the combined simulation of transient climate and transient atmospheric CO_2 . **b**, Relations of annual net primary production (NPP) and annual heterotrophic respiration (R_H) to annual precipitation in the combined simulation of transient climate and transient atmospheric CO_2 . Annual NPP is negatively correlated with annual mean temperature ($R = -0.51, P < 0.05$), and positively correlated with annual precipitation ($R = 0.73, P < 0.01$). Annual R_H is positively correlated with temperature ($R = 0.60, P < 0.01$), but not significantly correlated with precipitation.

whereas a positive NEP means that these ecosystems are a sink for atmospheric CO_2 .

Model results indicate that CO_2 'fertilization' of the vegetation of the Amazon increases NEP. Climate variability with CO_2 fertilization generally resulted in a higher annual NEP than did climate without CO_2 fertilization (Table 1). The strength of the CO_2 fertilization effect for the Amazon Basin was between 0.1 to 0.4 Pg C yr⁻¹ for the 15-year period 1980–1994. The CO_2 effect includes both the direct stimulation of plant growth by CO_2 and the indirect enhancement of plant water use efficiency^{6,11}.

According to the TEM simulations, year-to-year variations in carbon storage are closely related to shifts among the phases of El Niño/Southern Oscillation. Undisturbed Amazonian ecosystems acted as a source of atmospheric CO_2 (that is, negative NEP) during El Niño years, 1982/1983, 1987/1988 and 1991/1992. An El Niño event results in drier and warmer weather conditions for the Amazon Basin¹⁸. Both drier weather and warmer temperatures decrease NPP, and warmer temperatures increase R_H (Fig. 1). In

other years, which are wetter and cooler, terrestrial ecosystems in the Amazon Basin acted as a sink for atmospheric CO_2 (that is, positive NEP).

For the period of this study, interannual variations of NEP are correlated with the interannual variations of NPP. Annual NPP shows much larger variations than annual R_H (Table 1). A major controller of NPP in the Basin appears to be soil moisture, which is a function of precipitation and temperature. Soil moisture represents water availability to plants; it controls, in part, the transformation of organically bound soil nitrogen to inorganic soil nitrogen, the nitrogen most readily available to plants^{19,20}. Our analysis shows that an increase in precipitation leads to increases in soil moisture ($R = 0.73, P < 0.002$) and net nitrogen mineralization ($R = 0.56, P < 0.03$). The model results, indicating a close link between soil moisture and nitrogen mineralization, are consistent with field measurements made in the western Amazon¹⁹.

Consistency between model results and field measurements is essential for establishing the credibility of a model such as TEM. The results of TEM are in reasonable agreement with measurement-based estimates of: (1) short-term, site-specific NEP; and (2) field-based estimates of basin-wide carbon stocks in vegetation and soils. At three sites in the Basin, two forests^{4,21} and one savanna²², the technique of eddy covariance has been used to estimate net carbon exchange between these ecosystems and the atmosphere. We ran TEM in site-specific mode for each place, using the climate for the period of the field study. The model-derived estimate was the same as the field estimate for the forest in Rondônia, western Amazon; 16% lower than the field estimate for the forest near Manaus in the central Amazon, and 22% lower than the field estimate for the savanna at the Reserva Ecológica de Águas Emendadas, Brazil (Table 2).

For the current climate and today's atmospheric CO_2 concentration, the TEM estimate of mean carbon density in the forest vegetation of the Basin is 14 kg C m⁻², which is within the range of 13.6 and 14.9 kg C m⁻² estimated from field surveys^{23,24}. Likewise, the mean Basin soil organic carbon density of 9.3 kg C m⁻², estimated with TEM, is close to the estimate of 10.3 kg C m⁻² based on the RADAM Brazil field survey²⁵.

Fan *et al.*²¹ have used their short-term, site-specific estimates of NEP to extrapolate to the forests of the whole Basin for 1987, and Grace *et al.*⁴ did the same for the period July 1992 to June 1993. Both groups^{4,21} estimated that the Basin's forests were acting as a major carbon sink: 1.2 Pg C yr⁻¹ for 1987 and 0.5 Pg C yr⁻¹ for the July 1992 to June 1993 period. In contrast, TEM simulations show the forests of the Basin to be a carbon source of -0.2 Pg C for 1987, and to be in balance for the period July 1992 to June 1993. The TEM results for the period July 1992 to June 1993 reflect the fact that the region was moving out of an El Niño in 1992, and into a neutral year in 1993. For the period July–December 1992, TEM indicated that the basin functioned as a strong carbon source (-0.6 Pg C); for the period January to June 1993, TEM showed that the Basin acted as a strong sink (0.6 Pg C).

The difference between the Basin-wide estimates of Fan *et al.*²¹ and Grace *et al.*⁴ and the ones from TEM is at least in part because both groups^{4,21} made the simplifying assumption that the vegeta-

Table 2 Modelled and field net ecosystem production estimates compared

Ecosystems/Location	Time period	Field-based estimate*	TEM-based estimate†	Refs
Tropical rain forests/Rondônia (10°05' S, 61°57' W)	May ~ June/93	0.6 g C m ⁻² d ⁻¹	0.6 g C m ⁻² d ⁻¹	4
Tropical rain forests/Manaus (2°56' S, 59°57' W)	April ~ May/87	0.6 g C m ⁻² d ⁻¹	0.5 g C m ⁻² d ⁻¹	21
Savanna/Emendadas (15°33' S, 47°36' W)	March ~ May/95	1.8 g C m ⁻² d ⁻¹	1.4 g C m ⁻² d ⁻¹	22

The field-based estimates for the two forest sites were average rates of net carbon exchange for the measurement periods. The field-based estimate for the savanna site was the maximum rate, the only rate reported by Miranda *et al.*²².

* The three field-based estimates of net ecosystem production were measured by the eddy covariance technique.

† We used gridded historical climate data as inputs to TEM for Rondônia and Emendadas. For Manaus, we use climate data from the site's weather station as inputs to TEM.

tion, soils and climate are uniform across the Basin for the period of interest. In contrast, the TEM estimates account for spatial variability of vegetation, soils and climate that give rise to place to place differences in NEP (Fig. 2). During El Niño years, annual NEP is negative at most sites in the Amazon Basin, but it does remain positive in some parts of the Basin, including the northwest corner. During non-El Niño years, most parts of the Basin have a positive annual NEP. Thus, site-specific NEP measurements made in the

field must be used with caution when extrapolating over space and time to develop Basin-wide estimates.

Several global-scale analyses have been undertaken to explore the relation between climate variability and carbon cycling. Kindermann *et al.*⁹ used a physiologically based model of the carbon budget in terrestrial ecosystems, the Frankfurt Biosphere Model (FBM), for the period 1980–1993; their general conclusions with respect to the tropical regions, defined as the latitudinal band from 30°N to 30°S, were that annual NEP of land ecosystems in the tropics is particularly sensitive to interannual variations in climate, and that interannual temperature variations cause the main effects on annual NEP, with precipitation variations being important in some places.

Although our analysis of the TEM results also indicates that NEP in tropical ecosystems of the Amazon Basin is sensitive to inter-annual climate variability, we suggest that changes in the amount and the timing of precipitation cause the main effects on annual NEP in this region. Our analysis further indicates that changes in precipitation combine with changes in temperature to affect soil moisture, the factor we have identified as an important controller of carbon storage in the Amazon Basin. This conclusion agrees well with field results from a forest near Manaus, Brazil²⁶.

With reference to the consequences for NEP of precipitation changes in the tropics, Kindermann *et al.*⁹ indicated that the drier tropical systems, including the drought deciduous forests, are affected most. Analysis of the TEM data for the major vegetation types in the Basin indicates that whereas changes in precipitation resulted in the largest relative changes in net carbon storage per unit area in the dry ecosystems, the largest absolute changes in net carbon storage per unit area occurred in the moist and wet forests of the Basin.

Braswell *et al.*¹⁰ investigated how interannual temperature variability affects net carbon storage in terrestrial ecosystems at the global scale and found a significant relationship between atmospheric CO₂ growth rate and temperature. Their analysis suggested that the terrestrial response to changes in temperature results in either enhanced plant production, reduced heterotrophic respiration, or both, such that global NEP is positive about two years after an El Niño event.

Our results for the Amazon region differ from the global analysis of Braswell *et al.*¹⁰. Although the TEM simulations indicate that both NPP and NEP are significantly correlated with ‘current’ air temperature and precipitation, our analyses indicate no significant two-year lag effect between temperature and NEP for undisturbed ecosystems in the Amazon Basin. This result is consistent with the fact that year-to-year temperature variations in the Basin are small. Combining the Braswell *et al.* analysis¹⁰ with ours, we infer that the two-year lag phenomenon must be occurring in the extra-tropical areas where El Niño events cause large increases in temperature⁵.

An additional issue is the long-term effect of interannual climate variability on regional and global carbon storage. Are carbon losses in some years balanced by carbon gains in others? Or is there any reason to believe that land ecosystems are on longer-term trajectories of carbon gain or loss? The TEM simulations suggest that during the fifteen-year period 1980–1994, the undisturbed ecosystems of the Amazon Basin accumulated a total of ~3.3 Pg C, or an average of ~0.2 Pg C yr⁻¹. The progressive increase in atmospheric CO₂ concentration is the factor most likely to be responsible for the accumulation (Table 1).

An average net carbon storage of 0.2 Pg C yr⁻¹ in the Basin has both regional and global implications. At the regional scale, a net storage of 0.2 Pg C yr⁻¹ is the same order of magnitude as the estimates of the net annual release of carbon to the atmosphere from deforestation in this region during the period from the 1970s to the 1990s^{12,27}. For the 1970s, Skole²⁷ estimated the release of carbon from the Brazilian Amazon to be 0.1 Pg C yr⁻¹ due to deforestation. For the early 1990s, Fearnside¹² estimated the defor-

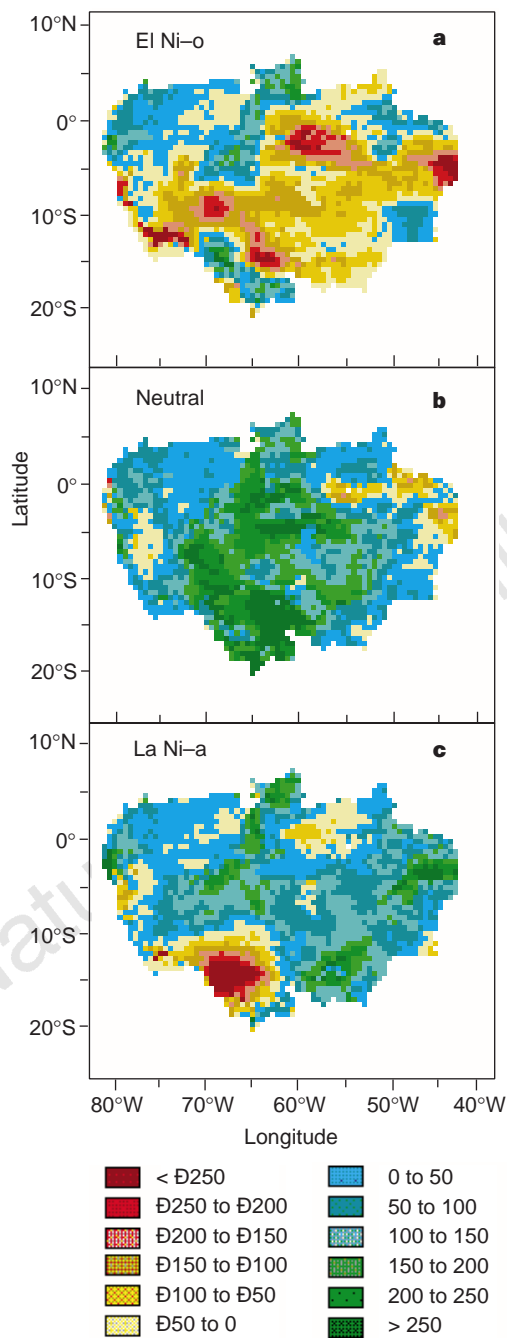


Figure 2 Net ecosystem production across the Amazon Basin. Spatial variability in net ecosystem production ($\text{g C m}^{-2} \text{yr}^{-1}$) in the combined simulation of transient climate and transient atmospheric CO₂ during three phases of El Niño/Southern oscillation: **a**, an El Niño year (1987); **b**, a neutral year (1981); and **c**, a La Niña year (1989). Regions that act as a source of atmospheric carbon (annual NEP is negative) are designated by shades of brown, red, or yellow, and regions that act as a sink of atmospheric carbon (annual NEP is positive) are designated by shades of blue or green.

estation-caused release of carbon from the Brazilian Amazon rose to 0.3 Pg. Thus, the TEM simulation suggests that releases of CO₂ from tropical deforestation in the Basin were partly balanced by CO₂ uptake by undisturbed ecosystems.

According to a recent IPCC analysis of the global carbon budget for the 1980s, terrestrial ecosystems were acting as a net sink for ~1.8 PgC per year⁷. The TEM simulation for the 1980s indicates that the undisturbed ecosystems in the Amazon Basin may have accounted for 13% of this terrestrial carbon sink. These decadal averages, of course, mask the effects of interannual climate variability on NEP in the world's terrestrial ecosystems. One of the next tasks is to check the results of global-scale analyses against measurements of well constrained global indexes of land-atmosphere carbon exchanges, such as the ratio of atmospheric N₂ to O₂ (ref. 28). Regional- and global-scale information on the spatial and temporal patterns of carbon uptake and release by terrestrial ecosystems, and the biogeochemical processes responsible for these patterns, are needed as we enter a post-Kyoto period in which we aim to manage the global carbon cycle.

Received 5 June; accepted 18 September 1998.

1. Melillo, J. M., Houghton, R. A., Kicklighter, D. W. & McGuire, A. D. Tropical deforestation and the global carbon budget. *Annu. Rev. Energy Environ.* **21**, 293–310 (1996).
2. Keller, M., Melillo, J. M. & de Mello, W. Z. Trace gas emissions from ecosystems of the Amazon basin. *Cienc. Cult. J. Braz. Assoc. Adv. Sci.* **49**, 87–97 (1997).
3. Melillo, J. M. *et al.* Global climate change and terrestrial net primary production. *Nature* **363**, 234–240 (1993).
4. Grace, J. *et al.* Carbon dioxide uptake by an undisturbed tropical rain forest in southwest Amazonia, 1992 to 1993. *Science* **270**, 778–780 (1995).
5. Nicholls, N. *et al.* in *Climate Change 1995: The Science of Climate Change* (eds Houghton, J. T. *et al.*) 132–192 (Cambridge University Press, Cambridge, UK, 1996).
6. Melillo, J. M., Prentice, I. C., Farquhar, G. D., Schulze, E.-D. & Sala, O. E. in *Climate Change 1995: The Science of Climate Change* (eds Houghton, J. T. *et al.*) 444–481 (Cambridge University Press, Cambridge, UK, 1996).
7. Schimel, D. S. *et al.* in *Climate Change 1995: The Science of Climate Change* (eds Houghton, J. T. *et al.*) 67–131 (Cambridge University Press, Cambridge, UK, 1996).
8. Dai, A. & Fung, I. Y. Can climate variability contribute to the “missing” CO₂ sink? *Glob. Biogeochem. Cyc.* **7**, 599–609 (1993).
9. Kindermann, J., Wurth, G., Kohlmaier, G. H. & Badeck, E.-W. Interannual variation of carbon exchange fluxes in terrestrial ecosystems. *Glob. Biogeochem. Cyc.* **10**, 737–755 (1996).
10. Braswell, B. H., Schimel, D. S., Linder, E. & Moore III, B. The response of global terrestrial ecosystems to interannual temperature variability. *Science* **278**, 870–872 (1997).
11. Tian, H., Melillo, J. M., Kicklighter, D. W., McGuire, A. D. & Helfrich, J. The sensitivity of terrestrial carbon storage to historical atmospheric CO₂ and climate variability in the United States. *Tellus* (in the press).
12. Fearnside, P. M. Greenhouse gases from deforestation in Brazilian Amazonia: net committed emission. *Climatic Change* **35**, 321–360 (1997).
13. Enting, I. G., Wigley, T. M. L. & Heimann, M. *CSIRO Div. Atmos. Res. Techn. Pap. No. 31*, 1–120 (1994).
14. Jones, P. D. Hemispheric surface air temperature variations: a reanalysis and an update to 1993. *J. Clim.* **7**, 1794–1802 (1994).
15. Hulme, M. *A Historical Monthly Precipitation Data Set for Global Land Area from 1900 to 1994*. Univ. East Anglia, Norwich, UK (1995).
16. Loveland, T. R. & Belward, A. S. The IGBP-DIS 1 km land-cover data set, DISCOVER—first results. *Int. J. Remote Sensing* **18**, 3291–3295 (1997).
17. Skole, D. & Tucker, C. J. Tropical deforestation and habitat fragmentation in the Amazon: satellite data from 1978 to 1988. *Science* **260**, 1905–1910 (1993).
18. Vörösmarty, C. J. *et al.* Analyzing the discharge regime of a large tropical river through remote sensing, ground-based climate data, and modeling. *Water Resources Res.* **32**, 3137–3150 (1996).
19. Neill, C. *et al.* Nitrogen dynamics in soils of forests and active pastures in the western Brazilian Amazon Basin. *Soil Biol. Biochem.* **27**, 1167–1175 (1995).
20. Melillo, J. M., Kicklighter, D., McGuire, A., Peterjohn, W. & Newkirk, K. in *Dahlem Conf. Proc.* 175–189 (Wiley, New York, 1995).
21. Fan, S. M., Wofsy, S. C., Bakwin, P. S. & Jacob, D. J. Atmosphere–biosphere exchange of CO₂ and O₃ in the central Amazon forest. *J. Geophys. Res.* **95**, 16851–16864 (1990).
22. Miranda, A. C. *et al.* Fluxes of carbon, water and energy over Brazilian cerrado: an analysis using eddy covariance and stable isotopes. *Plant. Cell Environ.* **20**, 315–328 (1997).
23. Brown, S. A. & Lugo, A. E. Aboveground biomass estimates for tropical moist forests of the Brazilian Amazon. *Interciencia* **17**, 8–18 (1992).
24. Fearnside, P. M. Forest biomass in Brazilian Amazonia: comments on the estimate by Brown and Lugo. *Interciencia* **17**, 19–27 (1992).
25. Moraes, J. F. L. *et al.* Soil carbon stocks of the Brazilian Amazon Basin. *Soil Sci. Soc. Am. J.* **59**, 244–247 (1995).
26. Williams, M. *et al.* Seasonal variation in net carbon exchange and evapotranspiration in a Brazilian rain forest: A modelling analysis. *Plant, Cell Environ.* (in the press).
27. Skole, D. *Measurement of Deforestation in the Brazilian Amazon Using Satellite Remote Sensing*. Thesis, Univ. New Hampshire (1992).
28. Keeling, R. F., Piper, S. C. & Heimann, M. Global and hemispheric CO₂ sinks deduced from changes in atmospheric O₂ concentration. *Nature* **381**, 218–221 (1996).

Acknowledgements. This work was supported by the Earth Observing System Program of the National Aeronautics and Space Administration and the Electric Power Research Institute through the Carbon Cycle Model Linkage Project (CCMLP) and the Vegetation/Ecosystem Modeling and Analysis Project (VEMAP). We thank M. Heimann and his coworkers at the Max Planck Institute, Hamburg, for climatic and CO₂ data, and C. Prentice, S. Brown, R. Huang, C. Neill and M. Williams for their critical comments.

Correspondence and requests for materials should be addressed to H.T. (e-mail: htian@lupine.mbl.edu).

Ratios of ferrous to ferric iron from nanometre-sized areas in minerals

Laurence A. J. Garvie* & Peter R. Buseck*†

* Department of Geology, † Department of Chemistry/Biochemistry, Arizona State University, Tempe, Arizona 85287-1404, USA

Minerals with mixed valence states are widespread and form in many different rock types¹. They can contain, for example, Fe²⁺–Fe³⁺ and Mn²⁺–Mn³⁺–Mn⁴⁺, with the ratios of oxidation states reflecting the redox conditions under which the host materials crystallized. The distribution of the ratio of iron (III) to total iron content (Fe³⁺/ΣFe) in minerals reflects the oxidation states of their host rocks and is therefore important for answering fundamental questions about the Earth's evolution and structure^{2–8}. Iron is the most sensitive and abundant indicator of oxidation state, but many mineral samples are too fine-grained and heterogeneous to be studied by standard methods such as Mössbauer spectroscopy, electron microprobe, and wet chemistry. Here we report on the use of electron energy-loss spectroscopy with a transmission electron microscope to determine Fe³⁺/ΣFe in minerals at the nanometre scale. This procedure is efficient for determining Fe³⁺/ΣFe ratios of minor and major amounts of iron on a scale heretofore impossible and allows information to be obtained not only from ultra-fine grains but also, for example, at reaction fronts in minerals.

Iron is abundant and occurs in oxidation states that range from Fe⁰ (for example, at the core–mantle boundary) to Fe³⁺ (at the Earth's surface). Estimates of the oxidation state of the Earth's upper mantle have been controversial, at least in part because of differences in the results produced by the various methods used to determine Fe³⁺/ΣFe values⁹. Mössbauer spectroscopy and wet chemical methods are bulk techniques, and do not provide information on fine-grained minerals or fine-scale heterogeneity. Micro-Mössbauer⁷, electron microprobe¹⁰, X-ray absorption^{11,12}, and X-ray photoelectron^{13,14} spectroscopies optimistically allow regions with diameters from 1 to 50 μm to be analysed. However, fine-grained heterogeneous samples and zoning at the sub-micrometre level

Table 1 Comparison of EELS and published Fe³⁺/ΣFe ratios

Sample	EELS		Published data	
	Fe ³⁺ /ΣFe	Fe ³⁺ /ΣFe	FeO _{tot}	Refs
Amphibole LC3*	0.75	0.76	11.08	28
Amphibole SC1*	0.52	0.49	16.69	28
Amphibole SC3*	0.31	0.26	16.83	28
Amphibole LC1*	0.65	0.63	10.96	28
Amphibole Kaert	0.93	0.93	11.82	29
Augite CVF1*	0.38	0.44	8.01	28
Augite PX4*	0.28	0.25	6.83	28
Augite SC4*	0.33	0.36	8.12	28
Augite SC6*	0.29	0.31	13.45	28
Augite LC4*	0.40	0.50	6.99	28
Glass 7‡	0.17	0.12	11.46	30
Glass 5‡	0.33	0.25	11.46	30
Glass air‡	0.82	0.70	11.46	30
Spinel KR35§	0.21	0.23 (0.29)	11.87	5

* Amphiboles LC1, LC3, SC1, SC3 and augites are from megacrysts in alkali basalts; Fe³⁺/ΣFe is from wet chemistry.

† Amphibole Kaert, Kaersutite from USNM no. 116503.0032. Fe³⁺/ΣFe is from Mössbauer spectroscopy.

‡ Glasses prepared from 1921 Kilauea basalt with CO/CO₂ gases at log f_{O₂} of –8, –7, –5 and in air at 1 atm and 1,400 °C; Fe³⁺/ΣFe is estimated from the activity–composition relationships in the system Fe–Pt.

§ Spinel from a mantle xenolith; Fe³⁺/ΣFe is from Mössbauer spectroscopy and, in brackets, microprobe data using the Bence–Albee data reduction method.